

The *In Situ* Formation of Giant Planets at Short Orbital Periods

A. C. Boley¹ A. P. Granados Contreras¹, and B. Gladman¹

Received _____; accepted _____

¹Department of Physics and Astronomy, The University of British Columbia, 6224 Agricultural Rd., Vancouver, B.C. V6T 1Z4, Canada

ABSTRACT

We propose that two of the most surprising results so far among exoplanet discoveries are related: the existences of both hot Jupiters and the high frequency of multi-planet systems with periods $P \lesssim 200$ days. In this paradigm, the vast majority of stars rapidly form along with multiple close-in planets in the mass range of Mars to super-Earths/mini-Neptunes. Such systems of tightly-packed inner planets (STIPs) are metastable, with the time scale of the dynamical instability having a major influence on final planet types. In most cases, the planets consolidate into a system of fewer, more massive planets, but long after the circumstellar gas disk has dissipated. This can yield planets with masses above the traditional critical core of $\sim 10 M_{\oplus}$, yielding short-period giants that lack abundant gas. A rich variety of physical states are also possible given the range of collisional outcomes and formation time of the close-in planets. However, when dynamical consolidation occurs before gas dispersal, a critical core can form that then grows via gas capture into a short-period gas giant. In this picture the majority of Hot and Warm Jupiters formed locally, rather than migrating down from larger distances.

Subject headings: planets and satellites: formation — planets and satellites: dynamical evolution and stability

1. INTRODUCTION

The existence of Hot and Warm Jupiters (HJ and WJ, respectively) has challenged planet formation theory since the discovery of these planet classes (Mayor & Queloz 1995; Marcy & Butler 1995). HJs are typically defined as planets with masses $\gtrsim 0.1M_J$ on orbits with periods P less than about 10 days (e.g., Gaudi et al. 2005; Wright et al. 2012). WJs are similar, but have orbits with longer periods out to the postulated water ice line (~ 1 AU). Together, HJs and WJs are members of a broader class of giant planets. We refer to any planet with a mass $> 10M_\oplus$ in the HJ/WJ regions as a short-period giant (SPG). We further use gSPG to distinguish any SPG that contains more than 50% of its mass in hydrogen and helium.

About 10% of FGK stars in the solar neighborhood harbor a giant planet at periods between 2 and 2000 days (Cumming et al. 2008; Howard 2013), with gSPGs comprising a large fraction of the sample. For example, approximately 1% of FGK stars in the solar neighborhood harbor an HJ (Marcy et al. 2005; Howard et al. 2012), making the HJ frequency about 1/10 of the total giant frequency (for the given periods). Under the classical paradigm of core nucleated instability (Pollack et al. 1996), gas giant planet formation becomes favorable at nebular distances that are cold enough to allow water ice to condense. Because the water ice line is thought to occur at distances of at least 1 AU from solar-type stars, strict adherence to this classical paradigm requires that gas giant planets migrate over one or two orders of magnitude in semi-major axis to explain the SPG population.

Instead of migration, one could question whether *in situ* gas giant formation is possible. This has been disfavored for various reasons, including: (1) The amount of condensable solids in the nebula's innermost region has been believed to be insufficient for reaching the critical core mass necessary for rapid gas capture (Lin et al. 1996). However, this is based on popular models of the solar nebula, which may not be correct or may not reflect a general property of exoplanetary systems (e.g., Chiang & Laughlin 2013). (2) The timescales required by core nucleated instability in the inner nebula are too long to explain the broad SPG population (Bodenheimer et al. 2000). (3) In the confirmed exoplanet catalogue, there had been a notable spike in the frequency of SPGs

at periods of about three days (the “3-day pileup”) followed by another rise in frequency near 1 AU (e.g., Cumming et al. 1999; Wright et al. 2009, 2011). This has been interpreted as evidence for migration, and is used as a test for different migration scenarios (e.g., Beaugé & Nesvorný 2012).

Here, we entertain the possibility that SPGs, including HJs, form *in situ*, motivated by advancements in exoplanet characterization and planet formation/evolution modeling.

Figure 1 shows the period distributions for planets and planet candidates with radii $R < 2R_J$ for three lower radii cuts, as well as $M \sin i > 0.1M_J$ for RV discoveries. These limits are chosen to select probable gas giant planets. The left panel uses the exoplanets.org database (Wright et al. 2011), excluding Kepler planet candidates, while the right panel uses only the Kepler database¹. The 3-day pileup is present in the confirmed planets in the full exoplanet database, which is dominated by transit surveys. In contrast, the rapid drop in SPG frequency for $P > 3$ days is not in the RV or Kepler data despite increasing bias against such detections. Moreover, using $0.6R_J < R < 2R_J$ for the Kepler sample, about half of the candidates are HJs and the other half are WJs (for periods less than 100 days), with no obvious break in the distribution. This highlights that the SPG formation mechanism does not, in general, produce a 3-day pileup.

We next consider Systems of Tightly-packed Inner Planets (STIPs), found in abundance in the Kepler catalogue. “Tightly-packed” refers to the systems having multiple planets within the same period space as HJs/WJs. N-body simulations demonstrate that STIPs are prone to decay, likely due to secular dynamics (Lithwick & Wu 2014; Pu & Wu 2015; Volk & Gladman 2015). The rate is logarithmic; roughly equal fraction of systems decay within equal logarithmic time intervals (Volk & Gladman 2015). If STIPs form early in the presence of gas, then for the small fraction of systems that rapidly become unstable, consolidation could produce the critical cores necessary to initiate runaway gas capture, which is feasible at short periods (e.g., Bodenheimer et al. 2000). Moreover, massive super-Earths/mini-Neptunes are expected to accrete significant gas within

¹Data obtained via exoplanets.org, August 2015.

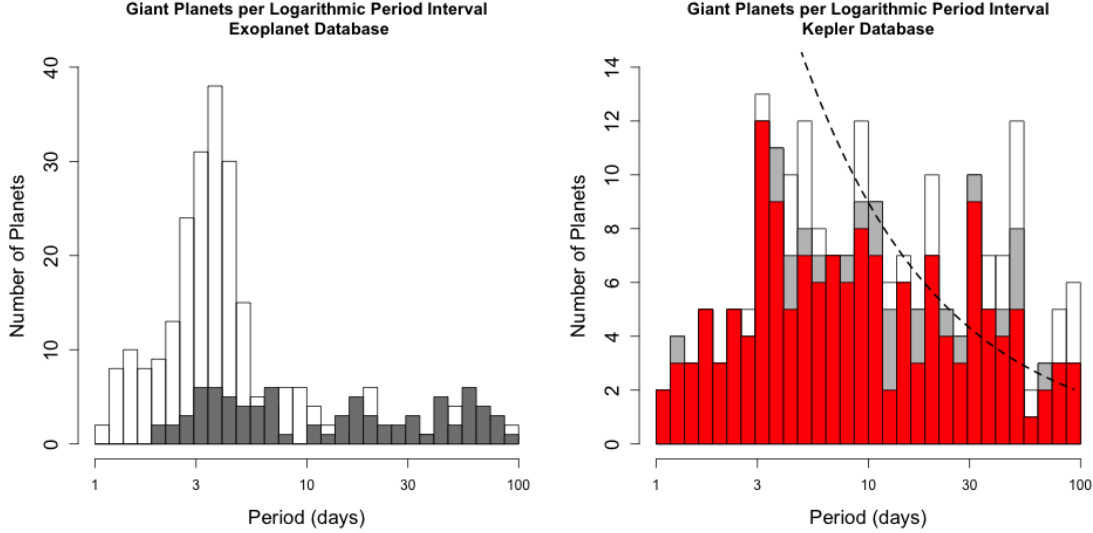


Fig. 1.— Distribution functions for planets in the exoplanet.org database. Left: The white histogram shows all confirmed planets with a measured or estimated size $0.6R_J < R < 2R_J$. The gray histogram shows all planets with $M \sin i > 0.1M_J$ discovered by the radial velocity method. Right: Kepler planets and planet candidates for three radii cuts. Coloring denotes planet sizes between $0.6R_J < R < 2R_J$ (white), $0.7R_J < R < 2R_J$ (gray), and $0.8R_J < R < 2R_J$ (red), demonstrating that the trend is independent of the lower bound used to represent the gas giant threshold. The 3-day pileup of HJs is only clearly present in the left panel white histogram, which is dominated by planets discovered by various transit surveys. In contrast, both the RV and Kepler discoveries continue steadily after periods of 5 days (with a slow decrease), *despite increasing bias against detection at longer periods*. To emphasize, the dependence of the single planet transit probability on orbital period P is illustrated by the dashed curve ($\propto P^{-2/3}$), assuming similar mass stars. The reason for this difference is not understood, as each survey has its own set of biases, but the above panels highlight that the 3-day pileup is not a general feature of (g)SPG formation.

disk lifetimes (Lee et al. 2014), regardless of their origin. As such, high-density super-Earths and planets with super-critical masses that never became gas giants (Marcy et al. 2014) are particularly challenging for the migration paradigm, as they should have accreted significant gas while migrating.

Here we suggest that gas-poor SPGs arise from consolidation after gas is removed, while gSPGs, including HJs, arise from the early consolidation of STIPs in the gaseous disk. We present n-body realizations of Kepler-11 as a case study to demonstrate the basic mechanism. We then place the results in a general picture that connects SPGs and low and high-density planets in STIPs to the conditions of the nebula at the time of STIP instability.

2. Numerical Experiments

We ran a series of n-body simulations to explore whether STIP decay could lead to SPG/gSPG formation. The following framework was used: (1) STIPs typically form with high planet multiplicity. As such, planetary systems with lower multiplicity are the decay products of these initial systems. (2) The high multiplicity STIPs observed today are representative of initial formation configurations, albeit the longest-lived variants. (3) STIPs form quickly, producing many planets in the Mars to mini-Neptune range ($< 10 M_{\oplus}$). While we expect a range of formation ages among STIPs, we assumed that all systems form well within 1 Myr of disk formation. We note that iron meteorite parent bodies in the Solar System formed within about 1.5 Myr of calcium-aluminum-rich inclusions (Scherstén et al. 2006) and that HL Tau appears to be well into the throes of planet formation after ~ 1 Myr, even at very large orbital distances. This picture thus seems plausible, but not guaranteed, as such short formation timescales for super-Earths/mini-Neptunes require high surface densities (Dawson et al. 2015). (4) The gaseous disk evolves rapidly, depleted on an exponential timescale of 2.5 Myr (e.g., Haisch et al. 2001; Mamajek 2009). (5) At early times, the natal disk has sufficient gas such that cores exceeding critical mass can grow to become gSPGs. Finally, (6) the critical core mass occurs at a single mass

($10 M_{\oplus}$ here). In detail, the critical mass depends on the local disk conditions and duration that gas is available (Lee & Chiang 2015; Piso et al. 2015), but the single mass allowed us to build a clean experiment.

We ran 1000 realizations of the Kepler 11 system (K11), which is intended to represent a *plausible* initial STIP architecture, not the only configuration; Volk & Gladman (2015) studied a larger set. We used K11 because the planetary locations and masses are well constrained, except the mass of the outermost planet, K11g. We set the K11g mass to be $8 M_{\oplus}$, which is comparable to other masses in the system and below both the derived upper mass limit (Lissauer et al. 2011) and the assumed critical core mass. As such, the planet masses and semi-major axes (M_{\oplus} , AU) are K11b = (1.9, 0.09), K11c = (2.9, 0.11), K11d = (7.3, 0.15), K11e = (8, 0.19), K11f = (2, 0.25), and K11g = (8, 0.47). The pericenter argument, ascending node longitude, and mean anomaly are uniformly distributed between 0 and 360 degrees. The eccentricities are uniformly random between 0 and 0.05, and the inclinations are drawn from a Rayleigh distribution with dispersion $\sigma = 1.8^{\circ}$ (Fabrycky et al. 2014). The inclination distribution is based on an analysis of the entire exoplanet population, while the eccentricity distribution is chosen for convenience in the absence of strong constraints on the low eccentricity regime.

All simulations were run using Mercury6 (Chambers 1999), modified to include a low-eccentricity correction for GR that captures the pericenter precession. Each realization is run for 20 Myr, well beyond the lifetime for most gaseous disks. We use the hybrid integrator, with a timestep of 0.1 days for the mixed-variable symplectic algorithm. During close approaches, which occur when planets pass within one Hill radius of another, the Burlirsch-Stoer algorithm is used, with an accuracy parameter of 10^{-12} .

3. Results

While the actual K11 is stable for Gyr timescales, of the 1000 realizations sampled here, 662 become unstable within 20 Myr. This large instability fraction is normal for STIPs (Volk &

Gladman 2015). Most mergers are between K11b and K11c, whose merged mass is below the $10 M_{\oplus}$ threshold. However, about 20% of the realizations produce at least one critical core, with about 4.4% of the collisions occurring within the first Myr. Two examples of consolidation outcomes are shown in Figure 2. In the first example, a four-planet system remains, with one critical core near the HJ period regime. In the second, two critical cores formed. Figure 3 highlights the fraction of systems that build at least one critical core, both per time interval and cumulative fraction.

To estimate whether gSPG formation could proceed following the formation of critical cores by consolidation, we introduce a gas decay timescale of 2.5 Myr (Mamajek 2009). The total gas mass among protoplanetary disks varies, but even a minimum mass solar nebula contains significant gas mass at short periods, with disk accretion feeding additional gas to the region. We set the start of the decay time ($t = 0$) to be commensurate with STIP formation (but see Dawson et al. 2015). In this model, $\exp\left(-\frac{t}{2.5 \text{ Myr}}\right)$ is the fraction of disks at time t that have enough gas to form a gSPG if a core appears. The red histograms in Figure 3, representing gSPG formation, are produced by weighting the open histograms in Figure 3 by the disk fraction for the corresponding time interval center. The cumulative fraction of systems that produce at least one gas giant over 20 Myr is about 6%, for our assumptions.

After a critical core appears, an additional ~ 1 Myr may be required before runaway gas accretion can occur (Lee et al. 2014). Such a delay would decrease the above gSPG formation to about 4%. However, recent work (Pfalzner et al. 2014) suggests that the disk exponential decay time is closer to 4 Myr. Using this decay time with the 1 Myr delay brings the total gSPG formation back to about 6%.

4. Discussion

The HJ frequency in the solar neighborhood is $\sim 1\%$ (Wright et al. 2012), while it is about 0.5% for the Kepler sample (Howard et al. 2012). The total Jupiter-type planet frequency around FGK

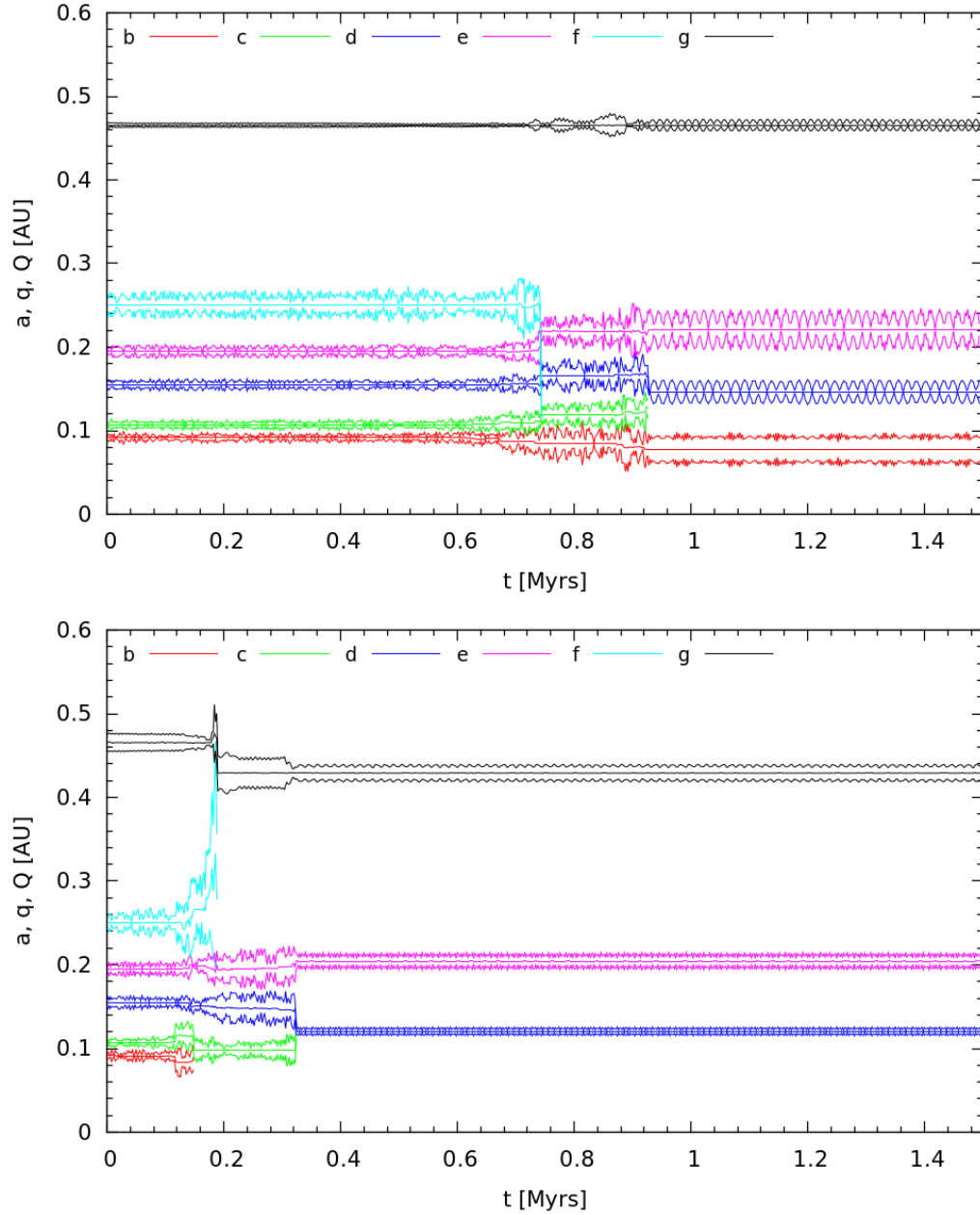


Fig. 2.— The semi-major axes a , pericentre q , and apocentre Q as a function of time for two realizations of Kepler-11, exhibiting different dynamical evolutions. Top panel: the consolidation ($[K11c + K11f] + K11d$) of a STIP produces a four-planet system with one $12 M_{\oplus}$ critical core (blue curve). Bottom panel: a three-planet system is produced ($[K11b + K11c] + K11d$) and ($K11g + K11f$) with two critical cores (black and blue curves). These cores are produced early enough in the disk's lifetime, assuming prompt STIP formation, that substantial gas could still be present.

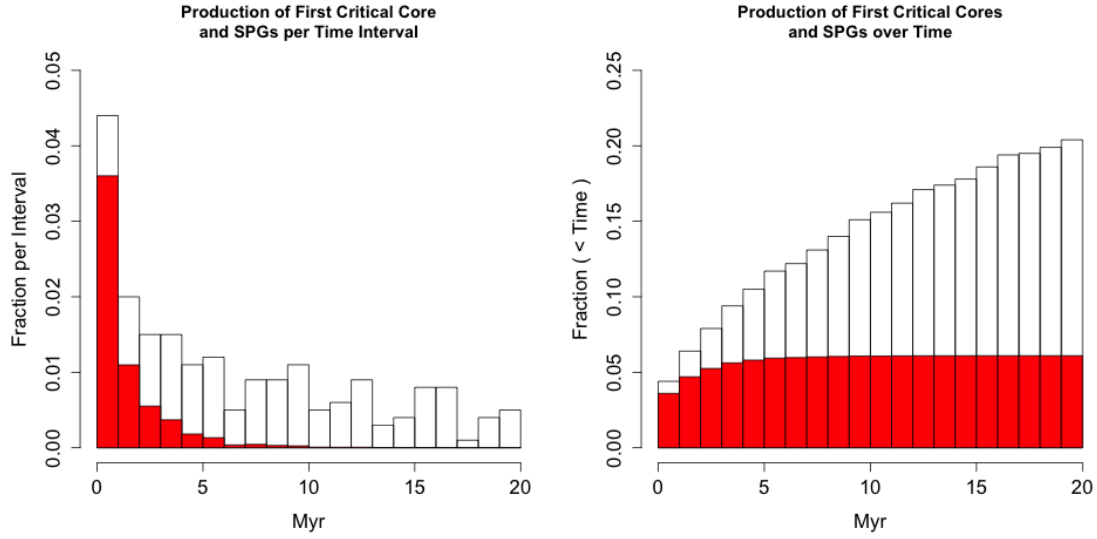


Fig. 3.— The open histograms show the fraction of systems (cumulative and per time interval) that produce a critical core. The red histograms are similar, but with each bin weighted by $\exp(-\frac{t}{2.5 \text{ Myr}})$, where t is the center of the given time interval. The exponential factor represents the observed decrease in disk accretion as a function of time, used here as a proxy for gas mass. Thus, the red histograms reflect gaseous short-period giant (gSPG) formation.

stars in the solar neighborhood (for periods less than 2000 days) is about 10% (Howard 2013), based on RV surveys. This includes giants at distances greater than 1 AU, where there is a rise in frequency per logarithmic period interval, possibly due to condensation of water ice (as classically viewed). The calculations here yield a gSPG occurrence of approximately 6%, comparable to the solar neighborhood gSPG frequency. If STIP instability produces SPGs, then the time of instability relative to gas depletion may be a principal factor in leading to gSPG formation versus a system of super-Earths/mini-Neptunes. This has been explored recently in the context of forming super-Earths with and without gas, where super-Earth/mini-Neptune formation in the presence of gas can lead to planets with low bulk densities (due to extended hydrogen atmospheres), while formation after gas dispersal can lead to higher-density planets (Dawson et al. 2015), even those larger than the critical core mass. Subsequent evolution, such as collisional or stellar-induced atmosphere evaporation can further add to the density diversity. The overall picture is shown in Figure 4.

Strictly, our K11 simulations do not produce a gas giant that would be classified as an HJ. This is a direct consequence of using K11 as the analogue system, which has the most massive cores at larger semi-major axes (relative to the HJ threshold). If the K11 planets were on slightly smaller orbits, then some of the gSPGs would potentially be HJs. The purpose of these calculations is to demonstrate that local STIP instability could form critical cores, not specifically to match the period distribution, which requires knowing the unknown initial planet population.

Regardless of critical core production, local gSPG formation is only possible if sufficient gas is present. Consider the early solar nebula as an example, with a surface density $\Sigma \propto r^{-1.5}$. The combined gas and solid mass between r_0 and r_1 is $M(r_0, r_1) \approx 2.4M_J \left(\frac{\Sigma_0}{1700 \text{ g cm}^{-2}} \right) (r_1^{0.5} - r_0^{0.5})$, where Σ_0 is the surface density at 1 AU and distances are in AU. The value $\Sigma_0 \sim 1700 \text{ g cm}^{-2}$ (Hayashi 1981) is often used in the literature, but may be insufficient to form Jupiter without spatially concentrating solids above the nominal condensible solid abundance (e.g., Lodders 2003); Σ_0 closer to $\sim 4000 \text{ g cm}^{-2}$ may be necessary for a *minimum* mass (Weidenschilling 1977; Kuchner 2004). Using this range for Σ_0 , the total mass from 0.05 AU to 0.5 AU is between ~ 1.2

and $2.7 M_J$ (about 2 and $4 M_{\oplus}$ of condensible silicates and metals). If one uses the exoplanet population to estimate protoplanetary disk masses (Chiang & Laughlin 2013), similar to that done for the solar nebula, then many systems had much higher available mass (in both solids and gas). Local formation of gas giants could proceed provided that the gas reservoir can be delivered to the critical core. The detailed growth of the planet will depend on the mass accretion rate through the evolving disk and the interactions of the planet with that gas (e.g., Bodenheimer et al. 2000; Benz et al. 2014). The inferred gas accretion rates among classical T Tauri stars is $\dot{M} \sim 10^{-8} M_{\odot} \text{yr}^{-1}$ (Gullbring et al. 1998), which is a mass flux of $10 M_J \text{Myr}^{-1}$, suggesting significant gSPG growth is possible after initial formation.

This mechanism does not intrinsically address the formation of large stellar spin-orbit misalignments (e.g., Albrecht et al. 2012). The cause of the misalignment is not understood, but may result from interactions between the disk and the star (Lai et al. 2011), interactions between the disk and the system’s birth environment (Bate et al. 2010; Batygin 2012; Fielding et al. 2015), and/or dynamical interactions between the planets followed by tidal evolution (e.g., Nagasawa & Ida 2011; Fabrycky & Tremaine 2007).

Another potential problem is that while many gSPGs show evidence of having at least one companion, they are at much larger orbital distances (Knutson et al. 2014). As the collisional outcomes in Figure 2 show, super-Earth/mini-Neptune-type planets can be closely spaced to the critical core after its formation. However, as the core grows in mass to become a gSPG, subsequent dynamics may give rise to neighbor clearing.

The effects of gas-planet interactions are not included in these simulations. Eccentricity damping in an isothermal disk (e.g., Tanaka & Ward 2004) suggests that the damping time (for small eccentricities) is less than 1 yr for a $\sim 10 M_{\oplus}$ planet near 0.1 AU, depending on disk conditions. At face value, this implies that our calculations overestimate the fraction of STIPs that can become unstable in the presence of gas. However, classic type I planet-disk interactions are known to be too efficient to explain planet populations without accounting for additional gas physics or processes (Baruteau et al. 2014; Benz et al. 2014). If this also extends to eccentricity damping,

then gas may be unable to completely prevent STIP instability. This must be explored further.

Finally, the differences between the solar neighborhood and Kepler HJ frequencies, assuming both samples are representative, might be resolved by metallicity (Wright et al. 2012). A higher metallicity may result in initial STIPs that have higher masses or a higher planet multiplicity. It may also increase the fraction of stellar host disks that produce a STIP in the presence of significant gas, as high solid surface densities are needed for STIP formation before gas dissipation (Dawson et al. 2015). We cautiously note that in the simulations presented here, there is a tendency for the inner planets to collide first (noted by Volk & Gladman 2015, who investigated additional STIPs). If a metallicity increase enhances this tendency, then one expects a shift in the period distribution of critical cores toward shorter periods. Furthermore, in this picture, the increase in gas giant frequency at periods near 1 AU (Wright et al. 2012) would be understood as the classical gas giant formation bias, where water ice contributes significantly in promoting critical core formation. Even in these outer regions, gas capture may be initiated through consolidation of rocky-ice embryos. No significant migration of massive planets is needed under this paradigm. An additional consequence is that the presence of a gSPG does not preclude terrestrial planet formation near ~ 1 AU.

During the review of this manuscript, a complementary study by Batygin et al. (2015) was posted to the arXiv.

We thank Kat Volk, Scott Tremaine, and the anonymous referee for comments and discussions that improved this manuscript. ACB was funded, in part, by the Canada Research Chairs program. ACB and APGC acknowledge additional funding by The University of British Columbia and an NSERC Discovery grant. BG was funded, in part, by an NSERC Discovery Grant. This research made use of the Exoplanet Orbit Database at exoplanets.org and was enabled in part by WestGrid and Compute Canada Calcul Canada.

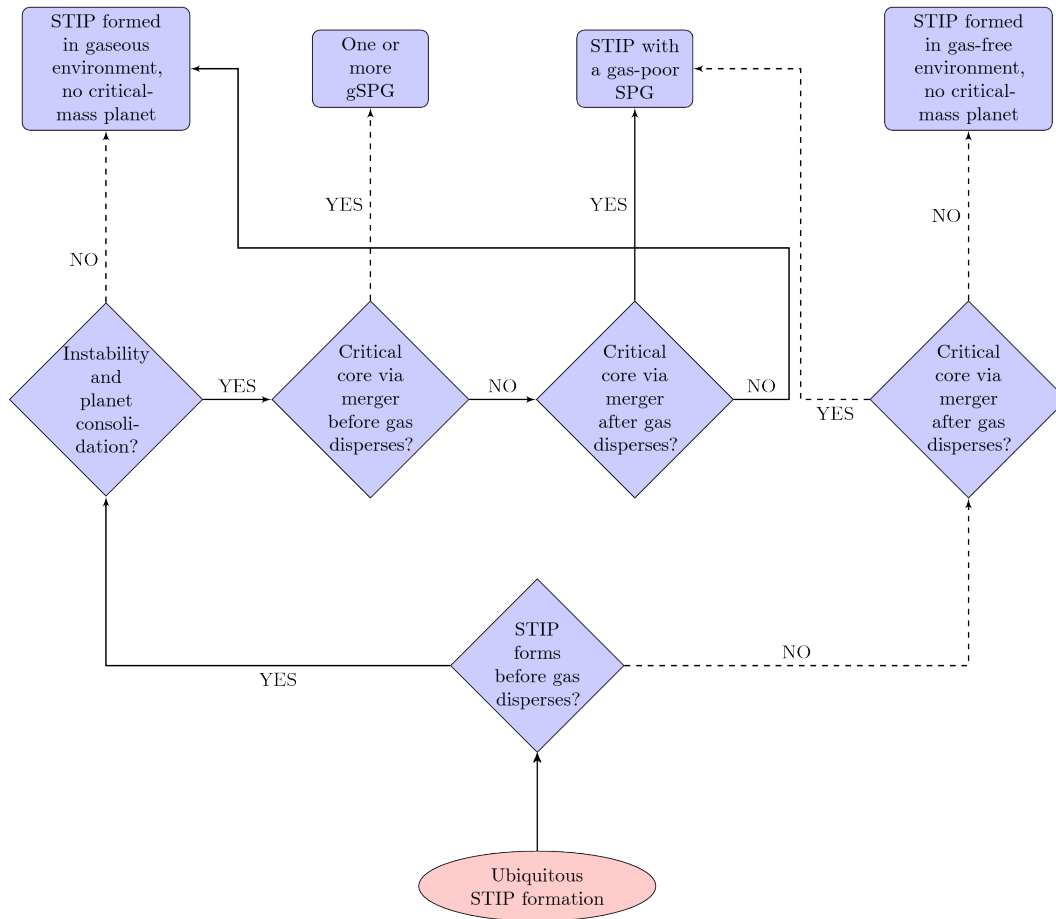


Fig. 4.— Formation paradigm for the diversity of planets at short orbital periods. Dashed lines correspond to paths that are envisaged to be rarer than solid lines. In this picture, consolidation plays a major role in determining planet populations. gSPG formation is possible if critical cores can form via system instability in the presence of gas. In contrast, if consolidation takes place after the gas has dissipated, then an SPG could form without leading to gas giant planet formation. Bulk densities will be affected by initial STIP mass and whether the STIP formed in the presence of gas. Subsequent processes, such as irradiation and giant impacts, can increase the diversity of densities even further.

REFERENCES

- Albrecht, S., Winn, J. N., Johnson, J. A., et al. 2012, *ApJ*, 757, 18
- Baruteau, C., Crida, A., Paardekooper, S.-J., et al. 2014, *Protostars and Planets VI*, 667
- Bate, M. R., Lodato, G., & Pringle, J. E. 2010, *MNRAS*, 401, 1505
- Batygin, K. 2012, *Nature*, 491, 418
- Beaugé, C., & Nesvorný, D. 2012, *ApJ*, 751, 119
- Benz, W., Ida, S., Alibert, Y., Lin, D., & Mordasini, C. 2014, *Protostars and Planets VI*, 691
- Bodenheimer, P., Hubickyj, O., & Lissauer, J. J. 2000, *Icarus*, 143, 2
- Chambers, J. E. 1999, *MNRAS*, 304, 793
- Chiang, E., & Laughlin, G. 2013, *MNRAS*, 431, 3444
- Cumming, A., Butler, R. P., Marcy, G. W., et al. 2008, *PASP*, 120, 531
- Cumming, A., Marcy, G. W., & Butler, R. P. 1999, *ApJ*, 526, 890
- Dawson, R. I., Chiang, E., & Lee, E. J. 2015, *MNRAS*, 453, 1471
- Fabrycky, D., & Tremaine, S. 2007, *ApJ*, 669, 1298
- Fabrycky, D. C., Lissauer, J. J., Ragozzine, D., et al. 2014, *ApJ*, 790, 146
- Fielding, D. B., McKee, C. F., Socrates, A., Cunningham, A. J., & Klein, R. I. 2015, *MNRAS*, 450, 3306
- Gaudi, B. S., Seager, S., & Mallen-Ornelas, G. 2005, *ApJ*, 623, 472
- Gullbring, E., Hartmann, L., Briceño, C., & Calvet, N. 1998, *ApJ*, 492, 323
- Haisch, Jr., K. E., Lada, E. A., & Lada, C. J. 2001, *ApJ*, 553, L153

- Hayashi, C. 1981, *Progress of Theoretical Physics Supplement*, 70, 35
- Howard, A. W. 2013, *Science*, 340, 572
- Howard, A. W., Marcy, G. W., Bryson, S. T., et al. 2012, *ApJS*, 201, 15
- Knutson, H. A., Fulton, B. J., Montet, B. T., et al. 2014, *ApJ*, 785, 126
- Kuchner, M. J. 2004, *ApJ*, 612, 1147
- Lai, D., Foucart, F., & Lin, D. N. C. 2011, *MNRAS*, 412, 2790
- Lee, E. J., & Chiang, E. 2015, *ApJ*, 811, 41
- Lee, E. J., Chiang, E., & Ormel, C. W. 2014, *ApJ*, 797, 95
- Lin, D. N. C., Bodenheimer, P., & Richardson, D. C. 1996, *Nature*, 380, 606
- Lissauer, J. J., Fabrycky, D. C., Ford, E. B., et al. 2011, *Nature*, 470, 53
- Lithwick, Y., & Wu, Y. 2014, *Proceedings of the National Academy of Science*, 111, 12610
- Mamajek, E. E. 2009, in *American Institute of Physics Conference Series*, Vol. 1158, American Institute of Physics Conference Series, ed. T. Usuda, M. Tamura, & M. Ishii, 3–10
- Marcy, G., Butler, R. P., Fischer, D., et al. 2005, *Progress of Theoretical Physics Supplement*, 158, 24
- Marcy, G. W., & Butler, R. P. 1995, in *Bulletin of the American Astronomical Society*, Vol. 27, American Astronomical Society Meeting Abstracts, 1379
- Marcy, G. W., Isaacson, H., Howard, A. W., et al. 2014, *ApJS*, 210, 20
- Mayor, M., & Queloz, D. 1995, *Nature*, 378, 355
- Nagasawa, M., & Ida, S. 2011, *ApJ*, 742, 72
- Pfalzner, S., Steinhausen, M., & Menten, K. 2014, *ApJ*, 793, L34

- Piso, A.-M. A., Youdin, A. N., & Murray-Clay, R. A. 2015, *ApJ*, 800, 82
- Pollack, J. B., Hubickyj, O., Bodenheimer, P., et al. 1996, *Icarus*, 124, 62
- Pu, B., & Wu, Y. 2015, *ApJ*, 807, 44
- Scherstén, A., Elliott, T., Hawkesworth, C., Russell, S., & Masarik, J. 2006, *Earth and Planetary Science Letters*, 241, 530
- Tanaka, H., & Ward, W. R. 2004, *ApJ*, 602, 388
- Volk, K., & Gladman, B. 2015, *ApJ*, 806, L26
- Weidenschilling, S. J. 1977, *Ap&SS*, 51, 153
- Wright, J. T., Marcy, G. W., Howard, A. W., et al. 2012, *ApJ*, 753, 160
- Wright, J. T., Upadhyay, S., Marcy, G. W., et al. 2009, *ApJ*, 693, 1084
- Wright, J. T., Fakhouri, O., Marcy, G. W., et al. 2011, *PASP*, 123, 412